

Subunit rotation in single FRET-labeled F₁-ATPase hold in solution by an anti-Brownian electrokinetic trap

Hendrik Sielaff^a, Thomas Heitkamp^a, Andrea Zappe^b, Nawid Zarrabi^b, Michael Börsch^{a,b,*}

^a Single-Molecule Microscopy Group, Jena University Hospital, Friedrich Schiller University Jena, Nonnenplan 2 - 4, 07743 Jena, Germany

^b 3rd Institute of Physics, University of Stuttgart, Pfaffenwaldring 57, 70550 Stuttgart, Germany

ABSTRACT

F₀F₁-ATP synthase catalyzes the synthesis of adenosine triphosphate (ATP). The F₁ portion can be stripped from the membrane-embedded F₀ portion of the enzyme. F₁ acts as an ATP hydrolyzing enzyme, and ATP hydrolysis is associated with stepwise rotation of the γ and ϵ subunits of F₁. This rotary motion was studied in great detail for the last 15 years using single F₁ parts attached to surfaces. Subunit rotation of γ was monitored by videomicroscopy of bound fluorescent actin filaments, nanobeads or nanorods, or single fluorophores. Alternatively, we applied single-molecule Förster resonance energy transfer (FRET) to monitor subunit rotation in the holoenzyme F₀F₁-ATP synthase which was reconstituted in liposomes. Now we aim to extend the observation times of single FRET-labeled F₁ in solution using a modified version of the anti-Brownian electrokinetic trap (ABELtrap) invented by A. E. Cohen and W. E. Moerner. We used Monte Carlo simulations to reveal that stepwise FRET efficiency changes can be analyzed by Hidden Markov Models even at the limit of a low signal-to-background ratio that was expected due to high background count rates caused by the microfluidics of the ABELtrap.

Keywords: F₁-ATPase; subunit rotation; single-molecule FRET; Hidden Markov Model; ABELtrap.

1 INTRODUCTION

F₀F₁-ATP synthase is an ubiquitous membrane protein that utilizes the electrochemical potential of protons over the membrane, that is the proton motive force (PMF), to synthesize adenosine triphosphate (ATP) from adenosine diphosphate (ADP) and inorganic phosphate (P_i). The bacterial enzyme can also work in reverse. Depending on the physiological conditions F₀F₁-ATP synthase hydrolyzes ATP in order to pump protons across the membrane^[1]. Here, we focus on the soluble F₁ portion where ATP hydrolysis takes place. In its simplest bacterial form F₁ consists of five different subunits, namely $\alpha_3\beta_3\gamma\delta\epsilon$. The structure of *Escherichia coli* F₁ was recently resolved by a crystal structure at a resolution of 3.15 Å (Fig. 1A)^[2,3]. The main body of F₁ consists of a pseudo-hexagonal structure formed by three pairs of subunits α and β , $\alpha_3\beta_3$. Each subunit β provides a nucleotide binding site that can bind and catalyze ATP synthesis or hydrolysis, while the corresponding nucleotide binding sites in each α subunit are catalytically inactive. Subunits $\alpha_3\beta_3$ together with subunit δ at the top of F₁ provide the rigid stator that stabilizes the complex^[4]. In contrast, subunits γ and ϵ form the central stalk which can rotate^[5]. The globular portion of subunit γ together with subunit ϵ connect to the membrane-embedded ring of *c*-subunits of the F₀ domain. On the other side the C- and N terminal α -helices of subunit γ intrude the $\alpha_3\beta_3$ pseudo-hexagon. Thereby, the holoenzyme can transfer the energy of the proton motive force generated in F₀ via rotational movements of *c*- ϵ - γ to the nucleotide binding sites in $\alpha_3\beta_3$, where it is transformed into chemical energy of ATP.

In order to maintain a high kinetic efficiency for energy conversion subunit γ must be elastically flexible^[6, 7]. It was shown that γ is at least ten times more flexible than the stator. The domain with highest elasticity is located at the interface to the *c*-subunits where the two rotor portions of F₀ and F₁ are connected^[8, 9]. Subunit γ transfers energy by its curved N-terminal α -helix to the DELSEED-sequence in subunit β , a helix-turn-helix motive, that interacts with the nucleotide binding site. Depending on the orientation of subunit γ the nucleotide binding sites are sequentially opened and closed, synchronizing binding and hydrolysis of ATP, and releasing the products ADP and P_i.

* Email: michael.boersch@med.uni-jena.de or m.boersch@physik.uni-stuttgart.de ; <http://www.m-boersch.org>

The exact sequence of events was revealed by a series of single molecule fluorescence microscopy experiments (see review^[10]). The $\alpha_3\beta_3\gamma$ part of F_1 was bound *via* Histidine-tags in each β subunit to the glass surface, while a fluorescent probe (actin filament, polystyrene bead, or magnetic bead) was attached on the opposite side of subunit γ to monitor its rotational movement during ATP hydrolysis. Subunit γ showed a 120° stepped rotation at high ATP concentrations corresponding to the three-fold symmetry of $\alpha_3\beta_3$. Furthermore, each 120° step consists of a 80° and a 40° substep^[11, 12]. In a sophisticated experimentally setup with additionally fluorescently labeled ATP the ATP binding reaction was correlated with the 80° substep. Further experiments showed that ATP is hydrolyzed in a pause between the two substeps, and that the 40° substep is related to the exergonic release of P_i from the nucleotide binding site. Finally ADP is released before the start of the next reaction cycle.

In order to prevent ATP hydrolysis *in vivo* the bacterial F_0F_1 -ATP synthase is thought to be regulated by subunit ϵ , a 15 kDa subunit which is part of the F_1 rotor^[13]. It consists of an N-terminal β -sandwich domain that binds to the globular domain of subunit γ and to the c -ring, and a C-terminal domain with two α -helices^[14, 15] in an 'extended'-configuration (Fig. 1A) or a distinct 'up'-configuration, respectively (Fig. 1B). It is considered to be an intrinsic inhibitor of the F_0F_1 -ATP synthase. However, in the active enzyme the C-terminal domain is thought to form a hairpin-folded state^[16] with the C-terminal helices in a 'down'-configuration (Fig. 1C). The two α -helices can extend parallel to subunit γ into the cavity of $\alpha_3\beta_3$, as shown by the crystal structures^[2, 17] (Fig. 1A and B), and thereby inhibit ATP hydrolysis activity by stalling the rotor at a fixed angle. A higher activation energy is needed to reactivate the enzyme from this ϵ -inhibited state than from another inhibited state, the so-called MgADP-inhibited state^[18]. Recently, an *E. coli* enzyme with a deleted C-terminal domain of subunit ϵ showed not only a higher ATP hydrolysis (ATPase) activity compared to the wild type, but also a higher ATP synthesis activity, that was not observed before^[19]. The authors suggest that the C-terminal domain in its extended form suppresses multiple elementary steps of the ATP synthesis or hydrolysis reactions that are executed in the three β subunits. In particular the C-terminal domain blocks the rotation of subunit γ , and, accordingly, all reactions that are accompanied by rotation, i.e. all rates of product release. On the other hand, the rates of covalent bond formation or cleavage of ATP are unaffected by subunit ϵ inhibition. In addition, biochemical experiments performed by S. D. Dunn and coworkers^[20] suggest that ϵ interacts also directly with the β subunits. Therefore it is believed that the physiological role of subunit ϵ is the inhibition ATP hydrolysis of the F_0F_1 -ATP synthase when the proton motive force and the ATP concentration in the cell are low to prevent waste of ATP.

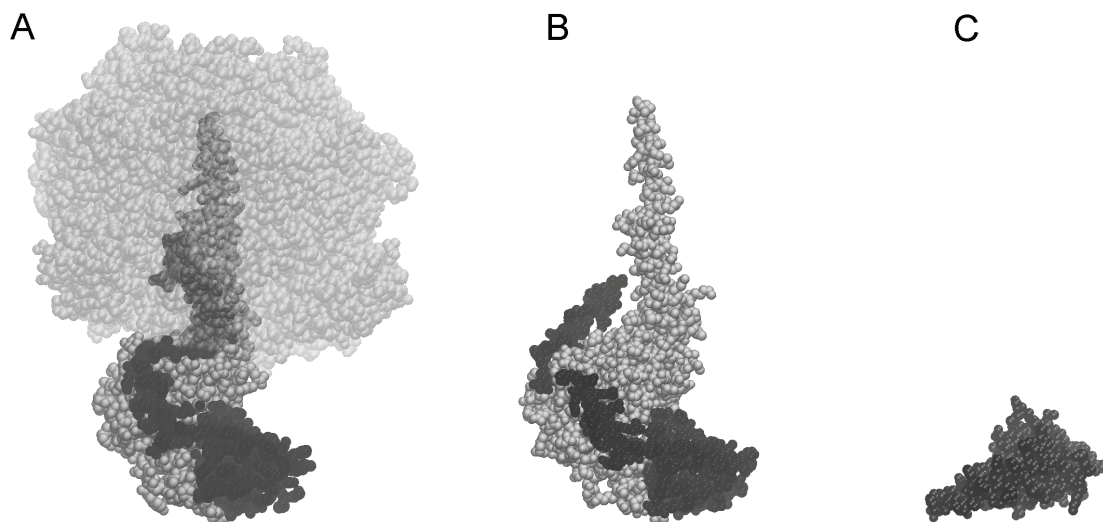


Figure 1. (A) Structure of *E. coli* F_1 with subunits $\alpha_3\beta_3$ in 'transparent' grey, γ in grey and ϵ in black^[2]. (B) Partial structure of the γ - ϵ subunits complex from *E. coli* with the C-terminal helices of ϵ in the 'up'-conformation^[21]. (C) Partial structure of the ϵ -subunit from *E. coli* F_1 with the C-terminal helices in the 'down'-configuration^[15].

Our group investigates conformational changes and subunit rotation in single F_0F_1 -ATP synthase using the Förster resonance energy transfer (FRET) approach since 1997^[22-51]. We have developed a specific FRET labeling scheme with both fluorophores attached to the F_1 portion to monitor rotation of subunit γ ^[24]. However, a major limitation of our confocal single-molecule FRET approach using freely diffusing, liposome-reconstituted F_0F_1 -ATP synthase is the short observation time, from of a few milliseconds for F_1 to some hundred milliseconds for reconstituted F_0F_1 . Recently we have built an Anti-Brownian Electrokinetic Trap (ABELtrap, invented by A. E. Cohen and W E Moerner) that can hold single small particles like 20-nm fluorescent beads for more than 8 seconds. These fast ABELtraps capture liposomes, DNA, proteins or even single fluorophores in solution^[52-54] with very fast feedback times in the microsecond time range^[55-59]. Here, we describe the current status of our F_1 -ATPase preparations for future single-molecule FRET measurements. We reveal the recovery of FRET levels by Hidden Markov Models (HMMs) at the lower limit of signal-to-background ratios, as expected in single-molecule FRET data using low laser excitation power for maximum observation times of the enzyme in the ABELtrap.

2 EXPERIMENTAL PROCEDURES

2.1 Preparation and characterization of F_1 -ATPase

The F_1 portion (F_1 -ATPase, F_1) of F_0F_1 -ATP synthase is prepared from the plasma membranes of *Escherichia coli*. Details of our actual preparation procedures are given below.

Construction of plasmid pMB3

Plasmid pMD2 (M. G. Düser, published in^[45]) is a derivative of pACWU1.2^[60] and carries a V78C mutation in the c -subunit and an N-terminal 6×Histidine-tag with the extension MRGS-HHHHHH-G- in the β -subunit of F_1 -ATPase. Plasmid pMB6 is a derivative of plasmid pRA100^[61] and carries a 56C point mutation in the ϵ -subunit^[27]. Plasmid pMD2 was digested with the restriction enzymes PmeI and SacI to yield a 548 bp long fragment carrying the 6×Histidine-tag at the N-terminus of subunit β . Plasmid pMB6 was digested with the same restriction enzymes, and a 12154 bp long fragment was isolated where the N-terminal sequence of the β -subunit was deleted. Both fragments were ligated resulting in the plasmid pMB3.

Bacterial strains and growth conditions

For the expression of the *E. coli* *atp* genes, strain RA1 (*F thi rpsL gal Δ(cyoABCDE)456::KAN Δ(uncB-uncC) ilv:Tn10*)^[62] was used, which lacks a functional F_0F_1 -ATP Synthase. This strain was transformed with the plasmid pMB3. Cells were grown in a modified complex medium (0.5 g/l yeast extract, 1 g/l tryptone, 17 mM NaCl, 10 mM glucose, 107 mM KH_2PO_4 , 71 mM KOH, 15 mM $(NH_4)_2SO_4$ and 4 μ M uracil, 50 μ M H_3BO_3 , 1 μ M $CoCl_2$, 1 μ M $MnCl_2$, 2 μ M $ZnCl_2$, 10 μ M $CaCl_2$, 3 μ M $FeCl_2$, 0.5 mM $MgSO_4$, 0.5 mM arginine, 0.5 mM isoleucine, 0.7 mM valine, 4 μ M thiamine, 0.4 μ M 2,3-dihydroxybenzoic acid) at 37° C in a 10 L FerMac 320 fermenter (Electrolab, UK), harvested in the late logarithmic phase, and pelleted in a Sorvall Evolution RC centrifuge (Thermo Fisher Scientific, USA) at 10,000 × g, 4 °C, for 5 min.

Purification of F_1 -ATPase using Histidine-tags

F_0F_1 -ATP synthase-containing membranes were purified and F_1 -ATPases were stripped off according to^[63] with some minor modifications. The cell lysis buffer contained 10 % (v/v) glycerol instead of the sucrose originally used. Furthermore, cells were lysed by two passages through a PandaPlus 2000 cell homogenizer (GEA Niro Soavi, Italy) at 1000 bar. Finally, instead of a PEG6000 precipitation, the soluble F_1 portion was precipitated by the addition of 65 % (v/v) saturated $(NH_4)_2SO_4$. The precipitated and pelleted F_1 was resuspended in buffer A (20 mM Tris-HCl pH 8, 300 mM NaCl, 1 mM $MgCl_2$, 5% (v/v) glycerol, 10 mM imidazole, 0.25 mM PMSF), loaded on a HisTrap FF column (GE-Healthcare, USA) equilibrated with buffer A, and connected to an Äkta PrimePlus FPLC system (GE-Healthcare, USA). After washing the column with five column volumes of buffer A, F_1 was eluted by an imidazole gradient over 20 column volumes up to 0.5 M imidazole in buffer A. F_1 -containing peak fractions were pooled and precipitated with 65 % (v/v) saturated $(NH_4)_2SO_4$. Pelleted F_1 was then resuspended in 0.5 ml buffer B (buffer A with 150 mM NaCl), and loaded on a Superdex 200 10/300 GL size exclusion chromatography column (GE-Healthcare, USA) equilibrated with buffer B and eluted using an Äkta PrimePlus FPLC system (GE-Healthcare, USA) with a flow rate of 0.5 ml/min.

The major peak fractions containing F_1 were pooled, concentrated using an Amicon Ultra-15 Ultracell 30K (Merck Millipore, USA), shock-frozen in liquid nitrogen in 500 μ l cryo straws, and stored at -80°C .

Measurement of ATP hydrolysis activity

ATPase activity was measured on the basis of established protocols^[64]. Briefly, 2 μ l of purified protein containing 1-2 μ g of the enzyme was added to buffer C (0.5 ml 50 mM Tris-Acetic acid pH 8.5, 10 mM ATP, 4 mM Mg-acetate), and incubated at 30°C for 5 min. The reaction was stopped by adding 0.5 ml of 10 % (w/v) SDS and the free phosphate was determined by measuring absorbance at 700 nm after adding 0.5 ml ferrous ammonium sulfate- H_2SO_4 ammonium molybdate reagent^[65]. Specific LDAO activation of ATPase activity was determined by adding 0.5 % (v/v) LDAO to the reaction mixture.

Other methods

Protein concentrations were determined using published methods^[66]. SDS-polyacrylamide gels were made as described^[67] with acrylamide concentrations between 12 - 14 %. Silver staining was performed according to^[68].

2.2 Simulation of FRET data mimicking subunit rotation in F_1 -ATPase

We aim at prolonged observation times of single FRET-labeled F_1 -ATPase in solution using an ABELtrap. To evaluate the minimum signal-to-background ratio required for subsequent FRET data analysis by Hidden Markov Models (HMMs), we simulated the stepwise rotation of subunit γ of F_1 using a Monte Carlo simulation. Therefore, a single FRET-labeled particle was placed into a virtual box. A threedimensional ellipsoid was centered within this box representing the threedimensional detection volume of a confocal experiment. Previously the FRET-labeled particle could diffuse freely in and out of the ellipsoid^[31]. Here, we changed the simulations so that the FRET-labeled particle was confined inside the ellipsoid as soon as it diffused into the boundaries of the ellipsoid. Depending on the given photophysical rates for photobleaching of the FRET donor and FRET acceptor dyes, the particle was forced to stay inside the ellipsoid until the fluorescence signal disappeared irreversibly. Subsequently the next freely-diffusing FRET-labeled particle was generated in the box but outside of the ellipsoid, and the ABELtrap simulation proceeded. Low photon count rates with shot-noise-limited intensity fluctuations plus a high background count rate on both detection channels were used yielding nearly constant count rates for the sum of both FRET donor and acceptor fluorescence photons.

2.3 Hidden Markov Model-based FRET level analysis

The simulated FRET time trajectories of a single particle in the ABELtrap were analyzed using previously described Hidden Markov Models (HMM) with the given number of 4 states. Three different FRET levels and one 'donor only' state (after FRET acceptor photobleaching) were expected. In contrast to our previous HMM approach to find FRET states in freely-diffusing proteoliposomes^[31, 34] we used Gaussian distributions for each FRET state with variable widths. After the first round of HMM learning the 3 FRET levels, the 'donor only' state and the associated dwell times, the resulting FRET levels and corresponding dwell times were used to assign these FRET levels (and the 'donor only' state) to the FRET time trajectories. The dwell time histograms of the assigned FRET levels were fitted with monoexponential decay functions to unravel the deviations between the learned HMM values and the assigned FRET levels.

3 RESULTS

The purification procedures of a fully active F_1 -ATPase from *E. coli* were established and described briefly. In contrast to our recently published F_0F_1 -ATP purification (T. Heitkamp et al., Proc. SPIE 8588 (2013)) which included the use of a new 10 L fermenter system for cell growth and a different type of cooled cell homogenizer to prepare the plasma membranes, we purified F_1 -ATPase with Histidine-tags using Ni-NTA column chromatography on an Äkta Prime Plus FPLC system. Cell membranes were collected after lysis of the cells by disruption at 1000 bar. The F_1 portion of the F_0F_1 -ATP synthase was purified from cell membranes in two steps. First, samples were loaded on a HisTrap column

binding the F₁-ATPase *via* its Histidine-tags in each β-subunit to the matrix of the column before elution with imidazole. In the second step, protein-containing fractions were applied to a size exclusion chromatography on a Superdex 200 column that served as a final polishing step to remove all remaining protein impurities. This procedure yielded F₁-ATPase of high purity as shown by SDS-PAGE in Fig. 2. The final protein sample contained only the F₁ subunits α, β, γ, δ, and ε, but not the F_o subunits *a*, *b*, and *c*. Most of the F_o subunits and other membrane proteins were stripped from the F₁ portion on the HisTrap column, where F₁ was bound to the column matrix, but not F_o. Now, single-molecule FRET experiments on the rotation of subunits γ and ε as well as the conformational changes of the C-terminus of ε are possible.

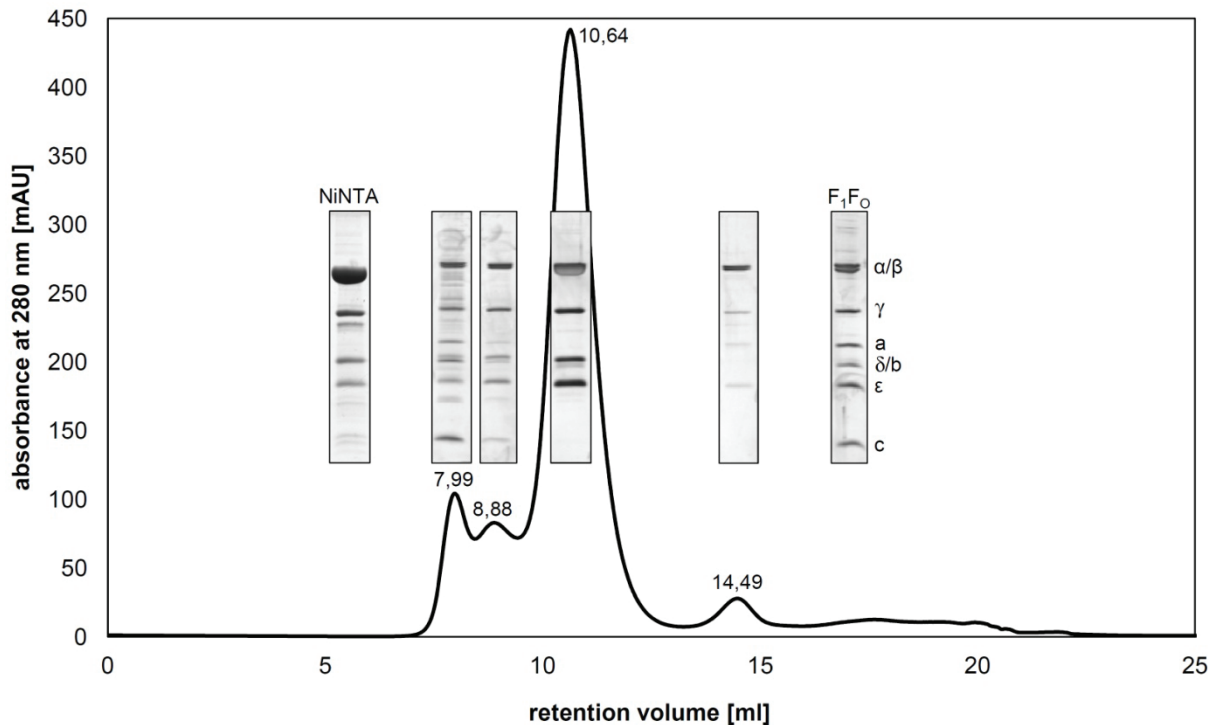


Figure 2. Purification profile of F₁-ATPase from *E. coli* (i.e. size exclusion chromatography after HisTrap column purification of F₁-containing fractions). Fractions with the highest protein concentrations were pooled, concentrated, and afterwards injected on a Superdex 200 column. The retention volumes of the peaks are indicated. Furthermore, the corresponding silver-stained SDS-PAGE of every peak fraction are shown. On the left, the SDS-PAGE of the injected sample is shown. The first protein peak (7.99 ml) corresponds to the void volume of the column and contained most of the impurities. The last protein peak on the right (14.49 ml) contained mainly the α and β subunits alone. The major peak contained F₁ with a high purity and without F_o subunits *a*, *b*, and *c*. The SDS-PAGE (see lane on the far right) shows a F_oF₁ standard for a better identification of the F₁ subunits α, β, γ, ε and δ.

ATP hydrolysis activities (ATP turnover) of the purified F₁-ATPase were measured to reveal functionality. The activity was measured at 30° C with an assay that determines the concentration of the released phosphate photometrically. We found an activity for the wild type F₁-ATPase of about 260 s⁻¹, which is in the same range as published activities^[69].

The observation time of the freely diffusing F₁-ATPase is approximately in the range of 1 to 3 ms using a confocal detection volume with a size of a few femtoliters. An ABELtrap is required to obtain FRET time trajectories of single F₁ captured in solution that last for several seconds. However, trapping FRET-labeled F₁ is not enough. Photobleaching of FRET donor or acceptor fluorophores depends on the number of excitation cycles. We aim to extend these observation time limitations by applying a reduced laser excitation power. This will result in a low photon count rate of both fluorophores. Therefore, we had to verify that the low photon count rates in the FRET time trajectories can be

analyzed quantitatively using Hidden Markov Models. A Monte Carlo simulation of a single trapped FRET-labeled particle (like F_1) in a box was used to explore FRET data analysis with HMMs.

A single particle was placed inside a box with $2.6 \mu\text{m} \times 2.6 \mu\text{m}$ in x and y dimensions, and $13.2 \mu\text{m}$ in z dimension. The particle moved due to Brownian motion and according to its size of 10 nm. The confocal three-dimensional Gaussian detection volume with 5.8 fl ($0.65 \mu\text{m}$ for x- and y-radii, $3.3 \mu\text{m}$ for z radius) was centered inside the box. Once the particle hit these boundaries it was considered 'trapped' and emitted on average 10000 photons per second for the FRET donor fluorophore as well as for the FRET acceptor fluorophore. Three different FRET efficiencies were set, at proximity factors 0.3, 0.5, and 0.7, and with short dwell times of 10 ms per level. A preferred sequence of $0.3 \rightarrow 0.7 \rightarrow 0.5 \rightarrow 0.3 \rightarrow$ was used to mimic unidirectional rotary movement, or sequential conformational changes, respectively. Photobleaching of the FRET donor was simulated based on a mean emission of 20000 photons before bleaching, and of 15000 photons before bleaching for the FRET acceptor. On both detection channels a mean photon count rate of 10000 counts per second (10 kHz) was added, similar to a background observed in experimental ABELtrap data. Ten FRET trajectories with 60 s duration each were simulated resulting in total 252 photon bursts with 8466 states.

For the subsequent HMM analysis, we binned the FRET time trajectories with 1 ms per data point. Data visualization was achieved with the software 'burst_analyzer'^[28], and background correction was used with 10 kHz for both FRET donor and acceptor channels. The HMM with 4 states (3 FRET levels plus one 'donor only' state for particles with a photobleached FRET acceptor dye) were given, but no preferred sequence of states was implemented. The starting values of the HMM were set to proximity factors 0.2 (for 'donor only' state), 0.4, 0.6 and 0.8, with variances of 0.02 for each FRET level, and dwell times of 20 ms.

The result of the HMM after learning was promising. FRET levels were learned at 0.1133 (with variance 0.0018, that is the 'donor only' state), 0.3145 with variance 0.0083, 0.5028 with variance 0.0125, and 0.6892 with variance 0.0082. All FRET levels were found in very good agreement with the simulated values. The associated dwell times were learned with 3741 ms for the 'donor only' state, and 9.31 ms, 9.18 ms or 9.73 ms for the three FRET levels 0.31, 0.50 or 0.69, respectively. Again, the identification of the FRET levels was in very good agreement with the simulation.

The final step of the HMM approach is the assignment of these learned FRET levels and dwell times to the simulated FRET time trajectories. The results are shown in Fig. 3. The two examples of photon bursts in Fig. 3A and B were terminated by FRET donor photobleaching. In Fig. 3A, the FRET acceptor bleached before the donor, and the remaining 'donor only' state with apparent FRET efficiency around 0.1 became visible at the end of the time trajectory. The assignment of FRET levels by the HMM was in good agreement with the simulation despite the low count rates and the additional noise contribution after background corrections of the data. Manual assignment of FRET levels appeared to be difficult.

The FRET transition density plot^[70] showed three pronounced transitions (Fig. 3C). The transitions from FRET level 1 at 0.7 to the following FRET level 2 at 0.5, and from 0.5 to 0.3, and from 0.3 to 0.7 clearly indicated the existence of a preferred sequence. This was the same sequence as the simulated one. The alternative transitions, that is from 0.3 to 0.5 to 0.7 to 0.3 and so on, were not assigned very often.

The dwell time distributions for the three assigned FRET levels were fitted with monoexponential decay functions from the maximum of the distribution yielding dwell times of 11.0 ms for FRET level 0.3 and 11.8 ms for FRET level 0.7 (data not shown). For FRET level 0.5 the fit to the dwell time distribution in Fig. 3D resulted in (15.4 ± 0.5) ms, which is slightly longer than the given dwell time of 10 ms for these states. Nevertheless, the dwell times were learned correctly by the HMM, and the subsequent assignment procedure prolonged the dwells due to missing some short dwell of a few milliseconds.

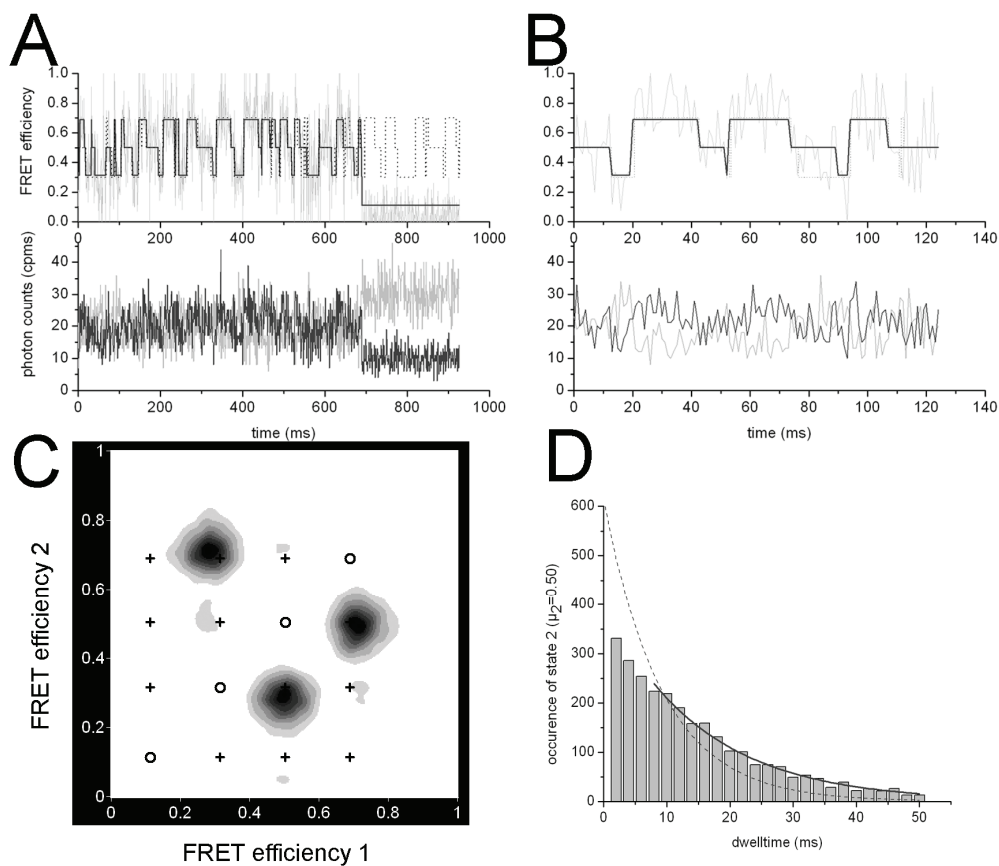


Figure 3. Simulated FRET data and FRET level recovery by a 4-state Hidden Markov Model. **(A)** Simulated FRET trajectory with FRET donor (grey line) and acceptor (black line) counts rates in counts per ms (cpms) in the lower panel, and the FRET efficiency trace in the upper panel. Recovered FRET levels are shown by the solid black line, simulated FRET levels by the dotted line. FRET acceptor photobleaching occurred after about 700 ms. **(B)** Simulated FRET trajectory with FRET donor and acceptor counts rates (lower panel) and FRET efficiency trace (upper panel). Assigned FRET levels are shown as a black line, simulated FRET levels as a dotted line. FRET donor photobleaching occurred after about 130 ms and terminated the photon burst. **(C)** FRET transition density plot from assigned FRET levels with three transitions clearly indicating the FRET level sequence. Crosses represent the expected transitions according to the simulation, open circles indicate apparent transitions with no change in FRET efficiency. **(D)** Dwell time distribution for the assigned FRET level $\mu_2=0.50$ in all 252 simulated bursts. The solid line is a monoexponential fit to the distribution, the dotted line is the expected dwell time distribution from the simulation.

4 DISCUSSION

Conformational changes of soluble proteins like F_1 -ATPase can be monitored using two specifically attached fluorophores for an internal distance ruler based on FRET. Because surface attachment might perturb the conformational dynamics, single-molecule FRET data are measured in solution. However, the observation time of a 10-nm sized enzyme in a confocal detection volume is less than 5 ms due to Brownian motion. Therefore, time trajectories with several FRET transitions cannot be recorded in general.

We are interested in long time trajectories of FRET changes in F_1 -ATPase for direct comparison with the holoenzyme, that is a liposome-reconstituted F_0F_1 -ATP synthase, as well as with other ATP-driven membrane transporters^[71-79]. As

the first step we established a purification protocol for F₁-ATPase from *E. coli*. Histidine-tags added to the N-terminus of the β -subunits and the corresponding Ni-NTA-based chromatography were used for purification. The purified F₁ contained all five subunits and showed good ATP hydrolysis activity. Because we had shown previously how to label F₁ specifically with two fluorophores for FRET-based rotation measurements^[24], we proceeded with improving single-molecule FRET analysis.

To identify the lower limit of the signal-to-background ratio for HMM-based FRET levels, we simulated FRET time trajectories with low photon count rates in the presence of a high background. These conditions were expected for capturing a single F₁-ATPase in solution by an ABELtrap^[80]. The ABELtrap is a microfluidic device keeping the enzyme within the confocal laser focus until photobleaching of the fluorophores. Diffusion of the enzyme is limited to the x- and y-directions within a 1- μ m shallow trapping region that is located between the cover glass and the PDMS chamber. Electrokinetic forces comprise electrophoretic and electroosmotic forces to counteract the actual movement of the protein in solution. Potentials are applied to four platinum electrodes to push back the protein to the center of the laser focus. We started with an ABELtrap approach using an EMCCD camera for particle localization^[81]. Recently we have built a faster ABELtrap using a confocal laser pattern which is controlled by a field-programmable gate array (FPGA). This ABELtrap could hold 20-nm fluorescent polystyrene beads in solution for more than 8 seconds, that is with 1000-fold prolongation of the observation time (N. Zarrabi et al, Proc. SPIE 8587 (2013), in press).

The Monte Carlo simulations for fast FRET level changes with mean dwell times of 10 ms per FRET level provided 252 photon bursts with 8466 FRET levels for HMM analysis. The high background on both channels added more noise on the photon count trajectories after it was subtracted. The given 4-state HMM for the three FRET levels plus the additional 'donor only' state recovered these FRET levels precisely, and also the learned dwell times matched the simulation. The subsequent assignment of the learned FRET levels and dwells yielded the correct FRET transitions and also the predefined FRET level sequence of the simulation. Minor deviations were found for the assigned dwell times. Obviously the assignment of very short FRET levels of a few milliseconds is difficult at low signal-to-background, and, accordingly, these FRET levels were overlooked.

Two different experimental requirements for future FRET analysis of freely diffusing F₁-ATPase have been achieved. The enzyme was purified with all subunits and was fully functional for ATP hydrolysis, and a low signal-to-background FRET data set could be analyzed successfully by Hidden Markov Models. Therefore, we expect that measuring conformational dynamics like subunit rotation of γ/ϵ or regulatory conformational changes of the C-terminus of ϵ will be possible soon. Long FRET time trajectories obtained in an ABELtrap will provide the required statistical basis for a quantitative description of the rates for these conformational dynamics, measured with one active enzyme at a time.

Acknowledgements

This work was supported in part by DFG grants BO 1891/10-2 and BO 1891/15-1 to M.B.. Additional financial support by the Baden-Württemberg Stiftung (by contract research project P-LS-Meth/6 in the program "Methods for Life Sciences") is gratefully acknowledged. The authors want to thank Prof. Dr. T. Duncan (SUNY Upstate Medical University, Syracuse, NY, USA), Prof. Dr. S. D. Dunn (University of Western Ontario, London, Ontario, Canada) and Prof. Dr. P. Gräber (University of Freiburg, Germany) for their support for F₁ and F₀F₁ mutants and enzyme purifications.

5 REFERENCES

- [1] Weber, J., and Senior, A.E., "Catalytic mechanism of F1-ATPase," *Biochim Biophys Acta* 1319, 19-58 (1997).
- [2] Cingolani, G., and Duncan, T.M., "Structure of the ATP synthase catalytic complex (F1) from *Escherichia coli* in an autoinhibited conformation," *Nat Struct Mol Biol* 18, 701-707 (2011).
- [3] Roy, A., Hutcheon, M.L., Duncan, T.M., and Cingolani, G., "Improved crystallization of *Escherichia coli* ATP synthase catalytic complex (F1) by introducing a phosphomimetic mutation in subunit epsilon," *Acta Crystallogr Sect F Struct Biol Cryst Commun* 68, 1229-1233 (2012).
- [4] Wachter, A., Bi, Y., Dunn, S.D., Cain, B.D., Sielaff, H., Wintermann, F., Engelbrecht, S., and Junge, W., "Two rotary motors in F-ATP synthase are elastically coupled by a flexible rotor and a stiff stator stalk," *Proc Natl Acad Sci U S A* 108, 3924-3929 (2011).
- [5] Zhou, Y., Duncan, T.M., Bulygin, V.V., Hutcheon, M.L., and Cross, R.L., "ATP hydrolysis by membrane-bound *Escherichia coli* F0F1 causes rotation of the gamma subunit relative to the beta subunits," *Biochim Biophys Acta* 1275, 96-100 (1996).
- [6] Cherepanov, D.A., Mulikjanian, A.Y., and Junge, W., "Transient accumulation of elastic energy in proton translocating ATP synthase," *FEBS Lett* 449, 1-6 (1999).
- [7] Junge, W., Panke, O., Cherepanov, D.A., Gumbiowski, K., Muller, M., and Engelbrecht, S., "Inter-subunit rotation and elastic power transmission in F0F1-ATPase," *FEBS Lett* 504, 152-160 (2001).
- [8] Sielaff, H., Rennekamp, H., Wachter, A., Xie, H., Hilbers, F., Feldbauer, K., Dunn, S.D., Engelbrecht, S., and Junge, W., "Domain compliance and elastic power transmission in rotary F(O)F(1)-ATPase," *Proc Natl Acad Sci U S A* 105, 17760-17765 (2008).
- [9] Junge, W., Sielaff, H., and Engelbrecht, S., "Torque generation and elastic power transmission in the rotary F0F1-ATPase," *Nature* 459, 364-370 (2009).
- [10] Okuno, D., Iino, R., and Noji, H., "Rotation and structure of FoF1-ATP synthase," *J Biochem* 149, 655-664 (2011).
- [11] Yasuda, R., Noji, H., Yoshida, M., Kinosita, K., Jr., and Itoh, H., "Resolution of distinct rotational substeps by submillisecond kinetic analysis of F1-ATPase," *Nature* 410, 898-904 (2001).
- [12] Bilyard, T., Nakanishi-Matsui, M., Steel, B.C., Pilizota, T., Nord, A.L., Hosokawa, H., Futai, M., and Berry, R.M., "High-resolution single-molecule characterization of the enzymatic states in *Escherichia coli* F1-ATPase," *Philosophical Transactions of the Royal Society B: Biological Sciences* 368, 20120023 (2013).
- [13] Nakanishi-Matsui, M., Kashiwagi, S., Hosokawa, H., Cipriano, D.J., Dunn, S.D., Wada, Y., and Futai, M., "Stochastic high-speed rotation of *Escherichia coli* ATP synthase F1 sector: the epsilon subunit-sensitive rotation," *J Biol Chem* 281, 4126-4131 (2006).
- [14] Uhlin, U., Cox, G.B., and Guss, J.M., "Crystal structure of the epsilon subunit of the proton-translocating ATP synthase from *Escherichia coli*," *Structure* 5, 1219-1230 (1997).
- [15] Wilkens, S., and Capaldi, R.A., "Solution structure of the epsilon subunit of the F1-ATPase from *Escherichia coli* and interactions of this subunit with beta subunits in the complex," *J Biol Chem* 273, 26645-26651 (1998).
- [16] Gibbons, C., Montgomery, M.G., Leslie, A.G., and Walker, J.E., "The structure of the central stalk in bovine F(1)-ATPase at 2.4 Å resolution," *Nat Struct Biol* 7, 1055-1061 (2000).
- [17] Hausrath, A.C., Capaldi, R.A., and Matthews, B.W., "The conformation of the epsilon- and gamma-subunits within the *Escherichia coli* F(1) ATPase," *J Biol Chem* 276, 47227-47232 (2001).
- [18] Saita, E., Iino, R., Suzuki, T., Feniouk, B.A., Kinosita, K., Jr., and Yoshida, M., "Activation and stiffness of the inhibited states of F1-ATPase probed by single-molecule manipulation," *J Biol Chem* 285, 11411-11417 (2010).
- [19] Iino, R., Hasegawa, R., Tabata, K.V., and Noji, H., "Mechanism of inhibition by C-terminal alpha-helices of the epsilon subunit of *Escherichia coli* FoF1-ATP synthase," *J Biol Chem* 284, 17457-17464 (2009).
- [20] Dunn, S.D., Tozer, R.G., and Zadorozny, V.D., "Activation of *Escherichia coli* F1-ATPase by lauryldimethylamine oxide and ethylene glycol: relationship of ATPase activity to the interaction of the epsilon and beta subunits," *Biochemistry* 29, 4335-4340 (1990).
- [21] Rodgers, A.J., and Wilce, M.C., "Structure of the gamma-epsilon complex of ATP synthase," *Nat Struct Biol* 7, 1051-1054 (2000).
- [22] Borsch, M., Turina, P., Eggeling, C., Fries, J.R., Seidel, C.A., Labahn, A., and Graber, P., "Conformational changes of the H⁺-ATPase from *Escherichia coli* upon nucleotide binding detected by single molecule fluorescence," *FEBS Lett* 437, 251-254 (1998).
- [23] Borsch, M., Diez, M., Zimmermann, B., Reuter, R., and Graber, P., "Stepwise rotation of the gamma-subunit of EF(0)F(1)-ATP synthase observed by intramolecular single-molecule fluorescence resonance energy transfer," *FEBS Lett* 527, 147-152 (2002).
- [24] Borsch, M., Diez, M., Zimmermann, B., Trost, M., Steigmiller, S., and Graber, P., "Stepwise rotation of the gamma-subunit of EFoF1-ATP synthase during ATP synthesis: a single-molecule FRET approach," *Proc. SPIE* 4962, 11-21 (2003).

- [25] Diez, M., Zimmermann, B., Borsch, M., König, M., Schweinberger, E., Steigmiller, S., Reuter, R., Felekyan, S., Kudryavtsev, V., Seidel, C.A., and Graber, P., "Proton-powered subunit rotation in single membrane-bound FoF1-ATP synthase," *Nat Struct Mol Biol* 11, 135-141 (2004).
- [26] Diez, M., Borsch, M., Zimmermann, B., Turina, P., Dunn, S.D., and Graber, P., "Binding of the b-subunit in the ATP synthase from *Escherichia coli*," *Biochemistry* 43, 1054-1064 (2004).
- [27] Zimmermann, B., Diez, M., Zarrabi, N., Graber, P., and Borsch, M., "Movements of the epsilon-subunit during catalysis and activation in single membrane-bound H(+)-ATP synthase," *Embo J* 24, 2053-2063 (2005).
- [28] Zarrabi, N., Zimmermann, B., Diez, M., Graber, P., Wrachtrup, J., and Borsch, M., "Asymmetry of rotational catalysis of single membrane-bound FoF1-ATP synthase," *Proc. SPIE* 5699, 175-188 (2005).
- [29] Zimmermann, B., Diez, M., Borsch, M., and Graber, P., "Subunit movements in membrane-integrated EFoF1 during ATP synthesis detected by single-molecule spectroscopy," *Biochim Biophys Acta* 1757, 311-319 (2006).
- [30] Zarrabi, N., Duser, M.G., Ernst, S., Reuter, R., Glick, G.D., Dunn, S.D., Wrachtrup, J., and Borsch, M., "Monitoring the rotary motors of single FoF1-ATP synthase by synchronized multi channel TCSPC," *Proc. SPIE* 6771, 67710F (2007).
- [31] Zarrabi, N., Duser, M.G., Reuter, R., Dunn, S.D., Wrachtrup, J., and Borsch, M., "Detecting substeps in the rotary motors of FoF1-ATP synthase by Hidden Markov Models," *Proc. SPIE* 6444, 64440E (2007).
- [32] Krebstakies, T., Zimmermann, B., Graber, P., Altendorf, K., Borsch, M., and Greie, J.C., "Both rotor and stator subunits are necessary for efficient binding of F1 to F0 in functionally assembled *Escherichia coli* ATP synthase," *J Biol Chem* 280, 33338-33345 (2005).
- [33] Duser, M.G., Bi, Y., Zarrabi, N., Dunn, S.D., and Borsch, M., "The proton-translocating a subunit of FoF1-ATP synthase is allocated asymmetrically to the peripheral stalk," *J Biol Chem* 283, 33602-33610 (2008).
- [34] Duser, M.G., Zarrabi, N., Cipriano, D.J., Ernst, S., Glick, G.D., Dunn, S.D., and Borsch, M., "36 degrees step size of proton-driven c-ring rotation in FoF1-ATP synthase," *Embo J* 28, 2689-2696 (2009).
- [35] Zarrabi, N., Ernst, S., Duser, M.G., Golovina-Leiker, A., Becker, W., Erdmann, R., Dunn, S.D., and Borsch, M., "Simultaneous monitoring of the two coupled motors of a single FoF1-ATP synthase by three-color FRET using duty cycle-optimized triple-ALEX," *Proc. SPIE* 7185, 718505 (2009).
- [36] Ernst, S., Duser, M.G., Zarrabi, N., and Borsch, M., "Three-color Förster resonance energy transfer within single FoF1-ATP synthases: monitoring elastic deformations of the rotary double motor in real time," *J Biomed Opt* 17, 011004 (2012).
- [37] Ernst, S., Duser, M.G., Zarrabi, N., Dunn, S.D., and Borsch, M., "Elastic deformations of the rotary double motor of single FoF1-ATP synthases detected in real time by Förster resonance energy transfer," *Biochimica et Biophysica Acta (BBA) - Bioenergetics* 1817, 1722-1731 (2012).
- [38] Steigmiller, S., Borsch, M., Graber, P., and Huber, M., "Distances between the b-subunits in the tether domain of F(0)F(1)-ATP synthase from *E. coli*," *Biochim Biophys Acta* 1708, 143-153 (2005).
- [39] Steigmiller, S., Zimmermann, B., Diez, M., Borsch, M., and Graber, P., "Binding of single nucleotides to H(+)-ATP synthases observed by fluorescence resonance energy transfer," *Bioelectrochemistry* 63, 79-85 (2004).
- [40] Steinbrecher, T., Hucke, O., Steigmiller, S., Borsch, M., and Labahn, A., "Binding affinities and protein ligand complex geometries of nucleotides at the F(1) part of the mitochondrial ATP synthase obtained by ligand docking calculations," *FEBS Lett* 530, 99-103 (2002).
- [41] Winnewisser, C., Schneider, J., Borsch, M., and Rotter, H.W., "In situ temperature measurements via ruby R lines of sapphire substrate based InGaN light emitting diodes during operation," *Journal of Applied Physics* 89, 3091-3094 (2001).
- [42] Boldt, F.M., Heinze, J., Diez, M., Petersen, J., and Borsch, M., "Real-time pH microscopy down to the molecular level by combined scanning electrochemical microscopy/single-molecule fluorescence spectroscopy," *Anal Chem* 76, 3473-3481 (2004).
- [43] Borsch, M., "Single-molecule fluorescence resonance energy transfer techniques on rotary ATP synthases," *Biological Chemistry* 392, 135-142 (2011).
- [44] Borsch, M., and Wrachtrup, J., "Improving FRET-based monitoring of single chemomechanical rotary motors at work," *Chemphyschem* 12, 542-553 (2011).
- [45] Galvez, E., Duser, M., Borsch, M., Wrachtrup, J., and Graber, P., "Quantum dots for single-pair fluorescence resonance energy transfer in membrane-integrated EFoF1," *Biochem Soc Trans* 36, 1017-1021 (2008).
- [46] Johnson, K.M., Swenson, L., Opipari, A.W., Jr., Reuter, R., Zarrabi, N., Fierke, C.A., Borsch, M., and Glick, G.D., "Mechanistic basis for differential inhibition of the F(1)F(o)-ATPase by aurovertin," *Biopolymers* 91, 830-840 (2009).
- [47] Seyfert, K., Oosaka, T., Yaginuma, H., Ernst, S., Noji, H., Iino, R., and Borsch, M., "Subunit rotation in a single F[sub o]F[sub 1]-ATP synthase in a living bacterium monitored by FRET," *Proc. SPIE* 7905, 79050K (2011).
- [48] Sielaff, H., and Borsch, M., "Twisting and subunit rotation in single FOF1-ATP synthase," *Phil Trans R Soc B* 368, 20120024 (2012).
- [49] Renz, M., Rendler, T., and Borsch, M., "Diffusion properties of single FoF1-ATP synthases in a living bacterium unraveled by localization microscopy," *Proc. SPIE* 8225, 822513 (2012).
- [50] Ernst, S., Duser, M.G., Zarrabi, N., and Borsch, M., "Monitoring transient elastic energy storage within the rotary motors of single FoF1-ATP synthase by DCO-ALEX FRET," *Proc. SPIE* 8226, 82260I (2012).

- [51] Hammann, E., Zappe, A., Keis, S., Ernst, S., Matthies, D., Meier, T., Cook, G.M., and Borsch, M., "Step size of the rotary proton motor in single FoF1-ATP synthase from a thermoalkaliphilic bacterium by DCO-ALEX FRET," *Proc. SPIE* 8228, 82280A (2012).
- [52] Cohen, A.E., and Moerner, W.E., "The anti-Brownian electrophoretic trap (ABEL trap): fabrication and software," *Proc. SPIE* 5699, 296-305 (2005).
- [53] Cohen, A.E., and Moerner, W.E., "An all-glass microfluidic cell for the ABEL trap: fabrication and modeling," *Proc. SPIE* 5930, 59300S (2005).
- [54] Cohen, A.E., and Moerner, W.E., "Method for trapping and manipulating nanoscale objects in solution," *Appl. Phys. Lett.* 86, 093109 (2005).
- [55] Cohen, A.E., and Moerner, W.E., "Controlling Brownian motion of single protein molecules and single fluorophores in aqueous buffer," *Opt Express* 16, 6941-6956 (2008).
- [56] Fields, A.P., and Cohen, A.E., "Electrokinetic trapping at the one nanometer limit," *Proc Natl Acad Sci U S A* 108, 8937-8942 (2011).
- [57] Goldsmith, R.H., and Moerner, W.E., "Watching conformational- and photodynamics of single fluorescent proteins in solution," *Nat Chem* 2, 179-186 (2010).
- [58] Bockenbauer, S., Furstenberg, A., Yao, X.J., Kobilka, B.K., and Moerner, W.E., "Conformational dynamics of single G protein-coupled receptors in solution," *J Phys Chem B* 115, 13328-13338 (2011).
- [59] Wang, Q., and Moerner, W.E., "An Adaptive Anti-Brownian Electrokinetic trap with real-time information on single-molecule diffusivity and mobility," *ACS Nano* 5, 5792-5799 (2011).
- [60] Kuo, P.H., Ketchum, C.J., and Nakamoto, R.K., "Stability and functionality of cysteine-less F(0)F1 ATP synthase from *Escherichia coli*," *FEBS Lett* 426, 217-220 (1998).
- [61] Aggeler, R., Chicas-Cruz, K., Cai, S.X., Keana, J.F.W., and Capaldi, R.A., "Introduction of reactive cysteine residues in the .epsilon. subunit of *Escherichia coli* F1 ATPase, modification of these sites with (azidotetrafluorophenyl)maleimides, and examination of changes in the binding of the .epsilon. subunit when different nucleotides are in catalytic sites," *Biochemistry* 31, 2956-2961 (1992).
- [62] Aggeler, R., Ogilvie, I., and Capaldi, R.A., "Rotation of a gamma-epsilon subunit domain in the *Escherichia coli* F1F0-ATP synthase complex. The gamma-epsilon subunits are essentially randomly distributed relative to the alpha3beta3delta domain in the intact complex," *J Biol Chem* 272, 19621-19624 (1997).
- [63] Wise, J.G., "Site-directed mutagenesis of the conserved beta subunit tyrosine 331 of *Escherichia coli* ATP synthase yields catalytically active enzymes," *J Biol Chem* 265, 10403-10409 (1990).
- [64] Senior, A.E., "Tightly bound magnesium in mitochondrial adenosine triphosphatase from beef heart," *Journal of Biological Chemistry* 254, 11319-11322 (1979).
- [65] Taussky, H.H., and Shorr, E., "A Microcolorimetric Method for the Determination of Inorganic Phosphorus," *Journal of Biological Chemistry* 202, 675-685 (1953).
- [66] Hartree, E.F., "Determination of protein: A modification of the lowry method that gives a linear photometric response," *Anal Biochem* 48, 422-427 (1972).
- [67] Schagger, H., and von Jagow, G., "Tricine-sodium dodecyl sulfate-polyacrylamide gel electrophoresis for the separation of proteins in the range from 1 to 100 kDa," *Anal Biochem* 166, 368-379 (1987).
- [68] Heukeshoven, J., and Dernick, R., "Simplified Method for Silver Staining of Proteins in Polyacrylamide Gels and the Mechanism of Silver Staining," *Electrophoresis* 6, 103-112 (1985).
- [69] Lobau, S., Weber, J., and Senior, A.E., "Catalytic site nucleotide binding and hydrolysis in F1F0-ATP synthase," *Biochemistry* 37, 10846-10853 (1998).
- [70] McKinney, S.A., Joo, C., and Ha, T., "Analysis of single-molecule FRET trajectories using hidden Markov modeling," *Biophys J* 91, 1941-1951 (2006).
- [71] Heitkamp, T., Kalinowski, R., Bottcher, B., Borsch, M., Altendorf, K., and Greie, J.C., "K(+)-Translocating KdpFABC P-Type ATPase from *Escherichia coli* Acts as a Functional and Structural Dimer," *Biochemistry* 47, 3564-3575 (2008).
- [72] Armbruster, A., Hohn, C., Hermesdorf, A., Schumacher, K., Borsch, M., and Gruber, G., "Evidence for major structural changes in subunit C of the vacuolar ATPase due to nucleotide binding," *FEBS Lett* 579, 1961-1967 (2005).
- [73] Verhalen, B., Ernst, S., Borsch, M., and Wilkens, S., "Dynamic ligand induced conformational rearrangements in P-glycoprotein as probed by fluorescence resonance energy transfer spectroscopy," *Journal of Biological Chemistry* 287, 1112-1127 (2012).
- [74] Diepholz, M., Borsch, M., and Bottcher, B., "Structural organization of the V-ATPase and its implications for regulatory assembly and disassembly," *Biochem Soc Trans* 36, 1027-1031 (2008).
- [75] Neugart, F., Zappe, A., Buk, D.M., Ziegler, I., Steinert, S., Schumacher, M., Schopf, E., Bessey, R., Wurster, K., Tietz, C., Borsch, M., Wrachtrup, J., and Graeve, L., "Detection of ligand-induced CNTF receptor dimers in living cells by fluorescence cross correlation spectroscopy," *Biochim Biophys Acta* 1788, 1890-1900 (2009).
- [76] Modesti, G., Zimmermann, B., Borsch, M., Herrmann, A., and Saalwachter, K., "Diffusion in Model Networks as Studied by NMR and Fluorescence Correlation Spectroscopy," *Macromolecules* 42, 4681-4689 (2009).
- [77] Ernst, S., Batisse, C., Zarrabi, N., Bottcher, B., and Borsch, M., "Regulatory assembly of the vacuolar proton pump VoV1-ATPase in yeast cells by FLIM-FRET," *Proc. SPIE* 7569, 75690W (2010).

- [78] Ernst, S., Schonbauer, A.K., Bar, G., Borsch, M., and Kuhn, A., "YidC-driven membrane insertion of single fluorescent Pf3 coat proteins," *J Mol Biol* 412, 165-175 (2011).
- [79] Ernst, S., Verhalen, B., Zarrabi, N., Wilkens, S., and Borsch, M., "Drug transport mechanism of P-glycoprotein monitored by single molecule fluorescence resonance energy transfer," *Proc. SPIE* 7903, 790328 (2011).
- [80] Fields, A.P., and Cohen, A.E., "Anti-Brownian traps for studies on single molecules," *Methods Enzymol* 475, 149-174 (2010).
- [81] Rendler, T., Renz, M., Hammann, E., Ernst, S., Zarrabi, N., and Borsch, M., "Monitoring single membrane protein dynamics in a liposome manipulated in solution by the ABELtrap," *Proc. SPIE* 7902, 79020M (2011).